Modeling the Organic Nitrate Yields in the Reaction of Alkyl Peroxy Radicals with Nitric Oxide. 1. Electronic Structure Calculations and Thermochemistry

Lawrence L. Lohr,[†] John R. Barker,*[,†,‡] and Robert M. Shroll[‡,#]

Department of Chemistry, University of Michigan, Ann Arbor, Michigan 48109-1055, and Department of Atmospheric, Oceanic, and Space Sciences, University of Michigan, Ann Arbor, Michigan 48109-2143

Received: March 12, 2003; In Final Form: June 20, 2003

Alkyl nitrates ($RONO_2$) are minor products formed in the atmospheric reactions of alkyl peroxy radicals (RO_2•) with nitric oxide. The major products are alkoxy radicals (RO•) and NO_2. The alkyl nitrate channel is important in the troposphere because $RONO_2$ formation results in removal of NO_x and trapping of free radicals; both effects reduce the rate of ozone production. We have used electronic structure calculations at the G3 and B3LYP/6-311++G** levels to calculate the geometries, energies, and vibrational frequencies for major stationary points on the potential energy surfaces for R = H, CH_3, C_2H_5, *n*-C_3H_7, *i*-C_3H_7, and 2-C_5H_{11}. Selected calculations have been made at the G2 and QCISD(T)/cc-pVTZ levels. Reaction energies are found to be rather insensitive to the size of the alkyl group. Corrections to the reaction energies are estimated, and a generic set of reaction energies are suggested. The B3LYP/6-311++G** barriers for the isomerization of ROONO to $RONO_2$ are found to be much too high to account for observed nitrate formation.

Introduction

The formation of alkyl and other organic nitrates by the reaction of peroxy radicals and NO has been the subject of several reviews.[1] Consider the reactions

$$RO_2\bullet + NO \rightarrow RO\bullet + NO_2 \quad (1a)$$

$$\rightarrow RONO_2 \quad (1b)$$

Reaction 1a converts relatively unreactive peroxy radicals (RO_2•) to highly reactive alkoxy radicals (RO•) and NO to NO_2. The NO_2 photolyzes in the troposphere to produce O, which in turn reacts with O_2 to produce O_3. Hence, reaction 1a leads to net O_3 production, while reaction 1b sequesters NO_x, reducing O_3 production. Recently measured[2] nitrate yields defined as $k_{1b}/(k_{1a} + k_{1b})$ are 0.141 ± 0.020, 0.178 ± 0.024, and 0.226 ± 0.032 for *n*-hexyl, *n*-heptyl, and *n*-octyl, respectively. These and earlier reported yields are a linear function of the number of C atoms for C_3-C_8. To develop a predictive model of alkyl nitrate yields defined as $k_{1b}/(k_{1a} + k_{1b})$, we have first carried out an extensive series of electronic structure calculations as described in this paper and reaction simulations as described in the following paper[3] in this issue using master equation techniques as incorporated in the MultiWell software package.[4]

A number of computational quantum chemical characterizations of peroxynitrites, nitrates, and their interconversion have been reported.[5−20] Particularly challenging has been the establishment of the preferred conformation of peroxynitrites. For example, studies[9] including electron correlation for HOONO have indicated the existence of at least four locally stable conformers, with the nature of the lowest energy conformer depending on the level of the computation. At correlated levels such as MP2/6-31G(d) and higher, the planar cis−cis conformer with C_s symmetry is favored, but only by about 4 kJ mol^{-1}, over a nonplanar cis-perp conformer, while at the noncorrelated HF/6-31G(d) level the nonplanar cis-perp conformer is slightly favored. In both of these conformers, the OONO portion of the molecule is either planar or nearly planar; in the cis-perp conformer the bond to H is nearly normal to this plane. The conclusion is that even simple peroxynitrites ROONO are likely to possess a number of locally stable conformers. (Even more conformers are expected if R is a large alkyl group.) Some of the conformers are likely to be close in energy; computational searches for isomerization pathways of peroxynitrites to the corresponding nitrates have to consider various possible starting structures. Indeed, a study[12] at the HF/6-31G* level of the rearrangement of HOONO to HNO_3 indicated that the intrinsic reaction coordinate (IRC) proceeds from trans-perp HOONO by lengthening of the O−O distance and migration of HO toward nitrogen. The nonplanar transition state was found to lie approximately 250 kJ mol^{-1} above HOONO and thus approximately 397 kJ mol^{-1} above HNO_3. The HOONO molecule itself was found to be approximately 42 kJ mol^{-1} lower in Gibbs energy (at 298 K) than the fragments NO + HO_2, but only 12 kJ mol^{-1} lower than NO_2 + OH.

A study closely related to our own is of Sumathi and Peyerimhoff who carried out a density functional theory (DFT) study[15] at the B3LYP/6-311++G** level of the potential energy surface for the HO_2 + NO reaction. Their value for the energy of the transition state for the isomerization of HOONO to $HONO_2$ is 163 kJ/mol including zero-point energy (ZPE) corrections. The transition state is a somewhat loose adduct of OH and NO_2 with an O−O distance between these fragments of 2.55 Å. At the single-point QCISD/6-311++G(2df,2pd)/MP2/6-311++G** level the barrier is even higher than at the DFT level, namely, 200 kJ mol^{-1}. At this same QCISD level, the dissociation energies of HOONO are 73.6 and 89.1 kJ mol^{-1} to form OH + NO_2 and HO_2 + NO, respectively. At the CAS-(8,8)/6-31G** level, the transition state is quite loose, with the O−O distance being 3.26 Å.

† Department of Chemistry.
‡ Department of Atmospheric, Oceanic, and Space Sciences.
# Present Address: Spectral Sciences, Inc., 99 S. Bedford St., Burlington, MA 01803-5169.

10.1021/jp034637r CCC: $25.00
Published on Web 08/20/2003

TABLE 1: Energy[a] of HOONO relative to $HONO_2$

level	$\Delta U°$ (0 K)	ref
B3LYP/6-311++G**	129.2	this work
G2	119.9	this work
G3	121.7	this work
QCISD(T)/cc-pVDZ	104.0	this work
QCISD(T)/cc-pVTZ[b]	111.2	this work
CCSD(T)/CBS	121.3	Dixon et al. (ref 17)
exp. estimate	114.1 ± 1	Hippler et al. (ref 22)

[a] Energy difference in kJ mol^{-1} including zero-point energies. [b] Energies evaluated at QCISD(T)/cc-pVDZ geometries.

Li and Francisco carried out a very thorough study[16] of the structure and stability of HOONO, obtaining at the QCISD(T)/cc-pVQZ level dissociation energies of 79 ± 4 and 105 kJ mol^{-1} to form OH + NO_2 and HO_2 + NO, respectively. Dixon et al.[17] followed this by examining various decomposition pathways for HOONO. They also reported a transition state for the isomerization of HOONO to $HONO_2$ having an energy at the CCSD(T)/ CBS//MP2/cc-pVDZ level (CBS denotes extrapolation of aug-cc-pVXZ results, X = D, T, Q, to the complete basis set limit) of 89.5 kJ mol^{-1} above that for HOONO and with a structure corresponding to a weakly bound adduct of OH and NO_2. (The distance from N to the O of OH is 2.784 Å.) At this same level the energy of OH + NO_2 is 82.8 kJ mol^{-1} above that of HOONO, so the isomerization transition state energy is slightly higher than that of these fragments. Rather different is the transition state for the methyl system recently located by Ellison et al.[18] On the basis of their coupled-cluster electronic structure calculations, there is a barrier of 80−120 kJ mol^{-1} for the isomerization of CH_3OONO to CH_3ONO_2, an energy not much below that for fragmentation to CH_3OO and NO. In a related study, Houk et al.[19] proposed on the basis of B3LYP/6-31G* calculations a loosely hydrogen bonded excited HOONO species as critical in the aqueous phase isomerization of HOONO to $HONO_2$. Zhang et al.[20] recently reported both quantum chemical and variational RRKM/master equation (vRRKM/ME) studies of the formation and isomerization of hydroxy peroxynitrites and nitrates as formed in the OH plus isoprene (C_5H_5) system. From their vRRKM/ME analysis, they conclude that the ROONO to RONO2 isomerization barrier lies within 1.6−4.6 kJ mol^{-1} below and 13.8−15.5 kJ mol^{-1} above the dissociation energy of ROONO to RO plus NO_2, a result consistent with our own conclusions.

$HONO_2$/HOONO Isomerization Energy. As an assessment of various computational levels, we present in Table 1 computed values of the energy difference between HOONO and $HONO_2$, with all values including zero-point energy contributions. All of our calculations were made using the Gaussian94 package[21] of quantum chemical programs. The DFT calculations employed the basis set 6-311++G**, also designated as 6-311++G(d, p), combined with the B3LYP functional to form the level B3LYP/6-311++G**. Compared to the recent experimental estimate of 114 ± 1 kJ mol^{-1} by Hippler et al.,[22] the DFT value is about 15 kJ mol^{-1} too high, while the G2 and G3 values are only about 7 kJ mol^{-1} too high, as is the CCSD(T)/CBS value of Dixon et al.[17] Somewhat too small is our QCISD(T)/cc-pVTZ//QCISD(T)/cc-pVDZ value. Our conclusion is that the B3LYP/6-311++G** level provides a reasonable estimate of the isomerization energy but not as good as the highly correlated wave function methods.

G3 and Density Functional Calculations. We have carried out an extensive series of G3 and DFT (B3LYP) calculations on molecular species of relevance to our study of alkyl nitrate yields from alkyl peroxy radicals in the atmosphere. The species considered are the alkoxy radicals RO, alkyl peroxy RO_2• radicals, alkyl peroxynitrites ROONO, and alkyl nitrates $RONO_2$, for the cases R = hydrogen (H), methyl (CH_3), ethyl (CH_3CH_2), *n*-propyl ($CH_3CH_2CH_2$), isopropyl ($(CH_3)_2CH$), and 2-pentyl (2-C_5H_{11}), as well as the fragments NO and NO_2. The calculated geometries and vibrational frequencies of the alkyl-substituted species are summarized in Table S-1 (Supporting Information). In the case of 2-pentyl only DFT calculations were made. The B3LYP density functional method employed is a hybrid method developed by Becke,[23] and represented by a three-parameter combination of Hartree−Fock, Becke 1998, and Slater exchange functionals together with the gradient corrected functional of Lee, Yang, and Parr (LYP). As recently discussed by He et al.,[24] this hybrid functional mimics pair and three-electron correlation effects which in wave function theory are only covered by coupled cluster methods. Lynch et al.[25] have commented on the remarkably high performance/cost ratio of this method for calculating accurate molecular structures, vibrational frequencies, and energetics, although they point out that reaction barrier heights are systematically underestimated in many cases. Cremer[26] has recently analyzed in detail the coverage of dynamic and nondynamic electron correlation effects in DFT methods, concluding that systems for which the reference state is a single-determinant state are described satisfactorily by standard DFT, while singlet biradicals and homolytically dissociating molecules are described very poorly. Thus, it is not surprising that the B3LYP method describes adequately the ROONO and $RONO_2$ equilibrium structures but not the loosely bound transition state connecting them along an isomerization pathway.

In Table 2 we present our B3LYP/6-311++G** and G3 values of $\Delta U°$ (0 K), $\Delta S°$ (298 K), and $\Delta G°$ (298 K) for the reaction types RO• + NO_2 → ROONO, RO• + NO_2 → $RONO_2$, RO_2• + NO → ROONO, and RO_2• + NO → RO• + NO_2. The $\Delta S°$ values designated as G3 are based on HF/6-31G(d) vibrational frequencies as computed within the G3 method, while the $\Delta G°$ values designated as G3 include these same $\Delta S°$ values as well as thermal corrections based on HF/6-31G(d) vibrational frequencies. With hydrogen and to some extent methyl as exceptions, both the G3 and DFT reaction energies are largely independent of the size of the R group involved. The G3 $\Delta U°$ (0 K) values are in every case considerably more negative than the B3LYP values for the three bond forming reactions but less negative for the oxygen exchange reaction RO_2• + NO → RO• + NO_2.

In Table 3 we present our G3 and B3LYP/6-311++G** values of $\Delta U°$ (0 K), $\Delta S°$ (298 K), and $\Delta G°$ (298 K) for the isomerization reaction ROONO → $RONO_2$ as well as B3LYP/6-311++G** values for forming the transition state along this isomerization pathway. Unlike the bond forming energies, the G3 and DFT isomerization energies agree well with each other; again they are essentially independent of the size of the R group.

By following the intrinsic reaction coordinates (IRCs) we have shown that the hydrogen TS connects nitric acid, $HONO_2$, not to the *cis*−*cis* HOONO minimum but rather to the cis-perp minimum lying 1.9 kJ mol^{-1} higher at the B3LYP/6-311++G** level, while the methyl TS connects methyl nitrate, CH_3ONO_2, to *cis*-perp CH_3OONO. The ethyl, *n*-propyl, isopropyl, and 2-pentyl DFT transition states closely resemble both in energy and structure the methyl transition state. All may be described as singlet diradicals with structures corresponding to adducts between RO• and NO_2 moieties. The values of the vibrational wavenumbers of the single imaginary frequency mode for each of the isomerization transition states are similar but decrease in

TABLE 2: Association Energies, Entropies, and Gibbs Free Energies

reaction	R	$\Delta U°$ (0 K)[a]	$\Delta S°$ (298 K)[b]	$\Delta G°$ (298 K)[c]
RO• + NO_2 → ROONO	H	−45.4 (−72.8)	−149.3 (−150.2)	−6.5 (−35.0)
	CH_3	−8.5 (−50.5)	−160.5 (−167.7)	36.4 (−4.3)
	CH_3CH_2	−16.1 (−56.1)	−162.1 (−170.3)	30.1 (−8.9)
	$(CH_3)_2CH$	−14.7 (−62.0)	−167.0 (−172.1)	33.8 (−13.5)
	$CH_3CH_2CH_2$	−14.1 (−54.1)	−163.8 (−174.2)	32.6 (−5.8)
	2-C_5H_{11}	−14.5	−167.7	33.7
RO• + NO_2 → $RONO_2$	H	−174.6 (−194.5)	−157.3 (−152.3)	−134.7 (−156.4)
	CH_3	−133.7 (−173.5)	−176.6 (−178.1)	−86.0 (−125.7)
	CH_3CH_2	−140.3 (−178.0)	−171.4 (−180.9)	−91.6 (−128.9)
	$(CH_3)_2CH$	−136.5 (−181.5)	−182.4 (−182.8)	−85.3 (−131.0)
	$CH_3CH_2CH_2$	−138.8 (−175.5)	−178.6 (−183.9)	−89.5 (−125.4)
	2-C_5H_{11}	−137.6	−180.8	−87.4
RO_2• + NO → ROONO	H	−84.1 (−108.8)	−165.3 (−166.7)	−40.2 (−65.9)
	CH_3	−74.3 (−98.8)	−163.4 (−163.7)	−30.0 (−54.4)
	CH_3CH_2	−74.0 (−100.2)	−165.2 (−164.0)	−28.2 (−55.4)
	$(CH_3)_2CH$	−75.0 (−102.2)	−162.6 (−162.0)	−29.6 (−56.9)
	$CH_3CH_2CH_2$	−73.8 (−101.6)	−167.0 (−165.2)	−27.5 (−56.5)
	2-C_5H_{11}	−74.2	−164.0	−29.9
RO_2• + NO → RO• + NO_2	H	−38.7 (−36.0)	−16.0 (−16.5)	−33.7 (−30.9)
	CH_3	−65.8 (−48.3)	−2.9 (4.0)	−66.4 (−50.1)
	CH_3CH_2	−57.9 (−44.0)	−3.1 (6.4)	−58.3 (−46.5)
	$(CH_3)_2CH$	−60.3 (−39.4)	4.4 (10.1)	−63.4 (−43.4)
	$CH_3CH_2CH_2$	−59.7 (−47.5)	−3.2 (9.0)	−60.1 (−50.7)
	2-C_5H_{11}	−59.7	3.7	−63.6

[a] Difference in electronic energies plus zero-point energies in kJ mol^{-1}. G3 values are in parentheses; all others are B3LYP/6-311++G** values. [b] Difference in molar entropies at 298 K and 1 atm in J K^{-1} mol^{-1}. HF/6-31G(d) values from G3 calculations are in parentheses; all others are B3LYP/6-311++G** values. [c] Difference in Gibbs free energies at 298 K and 1 atm in kJ mol^{-1}. G3 values are in parentheses; all others are B3LYP/6-311++G** values.

TABLE 3: Isomerization and Activation Energies, Entropies, and Gibbs Free Energies

reaction	R	$\Delta U°$ (0 K)[a]	$\Delta S°$ (298 K)[b]	$\Delta G°$ (298 K)[c]
ROONO → $RONO_2$	H	−129.2 (−121.7)	−7.9 (−2.0)	−128.2 (−121.4)
	CH_3	−125.2 (−123.0)	−16.1 (−10.4)	−122.4 (−121.4)
	CH_3CH_2	−124.2 (−121.8)	−14.7 (−10.6)	−121.7 (−120.0)
	$(CH_3)_2CH$	−121.7 (−119.5)	−15.4 (−10.7)	−118.9 (−117.5)
	$CH_3CH_2CH_2$	−124.8 (−121.4)	−14.8 (−9.7)	−122.1 (−119.6)
	2-C_5H_{11}	−123.2	−13.1	−121.1
ROONO → TS[d]	H	163.1	15.9	160.1
	CH_3	139.3	15.3	136.2
	CH_3CH_2	142.7	18.4	138.6
	$(CH_3)_2CH$	140.9	16.7	137.4
	$CH_3CH_2CH_2$	138.6	19.6	134.3
	2-C_5H_{11}	135.1	19.5	130.9

[a] Difference in electronic energies plus zero-point energies in kJ mol^{-1}. G3 values are in parentheses; all others are B3LYP/6-311++G** values. [b] Difference in molar entropies at 298 K and 1 atm in J K^{-1} mol^{-1}. HF/6-31G(d) values from G3 calculations are in parentheses; all others are B3LYP/6-311++G** values. [c] Difference in Gibbs free energies at 298 K and 1 atm in kJ mol^{-1}. G3 values are in parentheses; all others are B3LYP/6-311++G** values. [d] Transition state connecting singlet ROONO to singlet $RONO_2$.

magnitude as the size and hence mass of the R group increases, namely, 690i, 550i, 538i, 515i, 490i, and 461i for hydrogen, methyl, ethyl, *n*-propyl, isopropyl, and 2-pentyl cases, respectively. All six of these transition states are characterized by nearly constant bond distances from the oxygen of the RO• group to the NO_2 moiety, namely, 2.53 to 2.59 Å to one of the O atoms of NO_2, 2.38 to 2.54 Å to the N of NO_2, and 2.55 to 2.74 Å to the other O of NO_2. The activation energies $\Delta U°$ (0 K) for the ROONO → $RONO_2$ isomerization reactions are remarkably constant, namely, 141 ± 2 kJ mol^{-1}, for the five alkyl cases considered, but much too high to account for appreciable alkyl nitrate formation from ROONO isomerization.

Entropies. In Table 4 we present entropies computed from DFT structures and vibrational frequencies together with experimental $S°_m$ values as available.[27] The agreement is quite good for OH, HO_2, NO, NO_2, and $HONO_2$, with differences of 0.3 J K^{-1} mol^{-1} or less. However, for CH_3ONO_2 our calculated $S°_m$ value is smaller than the NIST value[27b] of 318.5 J K^{-1} mol^{-1} by 18.2 J K^{-1} mol^{-1}, while our $CH_3CH_2ONO_2$ value $S°_m$ is smaller than the NIST value[27b] of 348.34 J K^{-1} mol^{-1} by 15.3 J K^{-1} mol^{-1}. The literature values are typically based on harmonic oscillator contributions calculated from observed high-

TABLE 4: Molar Heat Capacities and Entropies for Hydrogen and Methyl Peroxynitrites, Nitrates, and Fragments

species	symmetry	state	$C_{v,m}$ [a]	$S°_m$ [b]	$S°_m$ (exp)[c]
HOONO (*cis*−*cis*)	C_s	$^1A'$	52.6	274.4	
$HONO_2$	C_s	$^1A'$	45.1	266.5	266.4
HO	$C_{\infty v}$	^2P	20.8	184.0	183.7
HO_2	C_s	$^2A''$	26.3	228.8	229.0
CH_3OONO (*cis*-perp)	C_1	^1A	75.3	316.4	
CH_3ONO_2	C_s	$^1A'$	66.2	300.3	318.5
CH_3O	C_s	$^2A'$	32.8	237.1	
CH_3O_2	C_s	$^2A''$	44.3	268.9	
NO	$C_{\infty v}$	^2P	20.8	210.9	210.8
NO_2	C_{2v}	$^2A_1$	28.5	239.8	240.1

[a] Molar constant volume heat capacity at 298 K and 1 atm in J K^{-1} mol^{-1}. [b] Molar entropy at 298 K and 1 atm in J K^{-1} mol^{-1}. [c] Experimental molar entropies in J K^{-1} mol^{-1} from ref 27b.

frequency fundamentals together with an assumption of free internal rotors for selected degrees of freedom, thus overestimating the entropy. By contrast, our S°_m values are based on harmonic oscillator contributions from all modes, including hindered rotors, thus possibly underestimating the entropy. The two lowest frequency modes for CH_3ONO_2 with C_{2v} symmetry are both of type a″, an $-NO_2$ rotation with $\nu/c = 131$ cm^{-1} and a CH_3 rotation with $\nu/c = 193$ cm^{-1} (DFT values). If these two modes are described as hindered rotors with respectively 2- and 3-fold barriers having curvatures at their minima fitted to the DFT harmonic force constants, our DFT S°_m value rises from 300.3 to 302.1 J K^{-1} mol^{-1}. If these two modes are treated as free rotors our S°_m value becomes 318.6 J K^{-1} mol^{-1}, essentially identical to the NIST value[27b] of 318.5 J K^{-1} mol^{-1}. However, we believe that the correct description for CH_3ONO_2 is that involving two hindered rotors, as calculations[28-30] based on observed fundamentals for 16 modes plus assumed hindered rotors having barriers estimated from microwave data have yielded S°_m values of 301.9 and 302.0 J K^{-1} mol^{-1}, essentially identical to our hindered rotor value of 302.1 J K^{-1} mol^{-1}.

Reaction Energy Corrections. While energy differences calculated with the B3LYP/6-311++G** method convincingly display a lack of any alkyl group dependence, the values themselves contain serious systematic errors which must be corrected before they can be employed in a reaction simulation. Dixon et al.[17] reported CCSD(T)/CBS dissociation energies including ZPEs estimated partly from experimental data for HOONO of 82.8 and 114.2 kJ mol^{-1} to form OH + NO_2 and HO_2 + NO, respectively, while our DFT ΔU° at 0 K values (Table 2) are 45.4 and 84.1 kJ mol^{-1}, respectively. Their value for the reaction HO_2 + NO → OH + NO_2 is -31.4 kJ mol^{-1}, the value from experimental[31] enthalpies of formation at 0 K is -31.6 kJ mol^{-1}, while our DFT value (combination of Table 2 values) is -38.7 kJ mol^{-1}. We reoptimized a QCISD/cc-pVTZ structure for $HONO_2$ provided to us by Francisco,[32] obtaining at the QCISD(T)/cc-pVTZ level a dissociation energy without zero-point corrections of 214.2 kJ mol^{-1} for $HONO_2$ to form OH + NO_2, a value 16.0 kJ mol^{-1} larger than the DFT value of 198.2 kJ mol^{-1}. Using the DFT ΔZPE value of -23.6 kJ mol^{-1} as an estimate, the QCISD(T)/cc-pVTZ value of ΔH° at 0 K becomes 190.6 kJ mol^{-1}, somewhat smaller than the 197.3 kJ mol^{-1} value from experimental[31] enthalpies of formation. (The DFT value including ΔZPE is much smaller, namely, 174.6 kJ mol^{-1}.)

These comparisons of DFT dissociation energies with those from higher level calculations and from experiments suggest the use of corrections of about 25 kJ mol^{-1} for the dissociation enthalpy of $HONO_2$ at 0 K to form OH and NO_2, 35 kJ mol^{-1} for the dissociation of HOONO to form OH and NO_2, and 35 kJ mol^{-1} for the dissociation of HOONO to form HO_2 and NO; the correction to the isomerization enthalpy of $HONO_2$ to HOONO is thus -10 kJ mol^{-1}. We have used these corrections for the hydrogen case as estimates of corrections to be applied to DFT energies for ethyl and higher alkyl cases. (Methyl DFT values of energies for reactions involving RO, as seen in Table 2, differ slightly from those for ethyl and higher.) Taking the $RONO_2$ energy as a fixed point, the energy of ROONO is reduced from its DFT value by 15 kJ mol^{-1}, that of RO• + NO_2 raised by 20 kJ mol^{-1}, and that of RO_2• + NO raised by 10 kJ mol^{-1}. These corrections, summarized in Table 5, place ROONO 110 kJ mol^{-1} above $RONO_2$, RO• + NO_2 160 kJ mol^{-1} above $RONO_2$, and RO_2• + NO 210 kJ mol^{-1} above $RONO_2$. As also seen in Table 5, these corrections bring the reaction energies nearly in line with our rounded off G3 values, the latter being the values we used in our reaction simultations[3] for the *n*-propyl and 2-pentyl systems.

TABLE 5: Generic Reaction Energies

reaction	R	ΔU° (0 K), DFT[a]	ΔU° (0 K), corr.[b]	ΔU° (0 K), G3[c]
$RONO_2 \rightarrow RO\bullet + NO_2$	H	175	200	195
	CH_3	135	155	175
	≥ CH_3CH_2	140	160	175
$ROONO \rightarrow RO\bullet + NO_2$	H	45	80	75
	CH_3	10	45	50
	≥ CH_3CH_2	15	50	55
$ROONO \rightarrow RO_2\bullet + NO$	H	75	110	110
	CH_3	75	100	100
	≥ CH_3CH_2	75	100	100

[a] Rounded-off differences in kJ mol^{-1} in B3LYP/6-311++G** electronic energies including zero-point energies. [b] Rounded-off differences in kJ mol^{-1} inB3LYP/6-311++G** electronic energies including zero-point energies and empirical corrections (see text). [c] Rounded-off differences in kJ mol^{-1} in G3 electronic energies including zero-point energies.

A serious concern is the very high barrier for the isomerization of ROONO to $RONO_2$ as found both in our calculations and in those of others. This barrier is a key parameter in our reaction simulation studies. We shall report[3] that to account for nonnegligible yields of the isopropyl and 2-pentyl nitrates it was necessary to assume that the barrier lies no higher than the energy of the exit channel to the oxy radical RO• and NO_2, a result not in agreement with our density functional (DFT) results but quite in line with the hydrogen system results of Dixon et al.,[17] implying that the barrier for the alkyl cases lies not more than about 50 kJ mol^{-1} above the energy of ROONO.

Elimination of HONO from $RONO_2$. On the basis of standard enthalpies of formation[27] the decomposition of methyl nitrate to form HONO and H_2CO is exothermic by 66.0 kJ mol^{-1}. Other alkyl nitrates are presumably also thermodynamically unstable with respect to decomposition to HONO and aldehydes. We have located a transition state with C_s symmetry on a pathway from eclipsed CH_3ONO_2 to HONO and H_2CO with an energy at the MP4SDTQ/D95(d,p)//HF/6-31G* level including HF/6-31G* zero-point contributions of 155.4 kJ mol^{-1} above that of the eclipsed nitrate or 163.3 kJ mol^{-1} above that of the more stable staggered nitrate. (This transition state has energies at the B3LYP/6-311++G** and G3 levels of 161.8 and 182.3 kJ mol^{-1}, respectively, above that of the staggered nitrate.) Similarly, we have located a transition state with C_1 symmetry for the decomposition of methyl peroxynitrite to the same products, HOONO and H_2CO, with energies at the B3LYP/6-311++G** and G3 levels of 163.5 and 180.7 kJ mol^{-1} above that of the peroxynitrite, respectively. On the basis of these high transition state energies, we conclude that the decomposition of alkyl nitrates and peroxynitrites to HONO and aldehydes are unlikely to play an important part in the reaction kinetics of alkyl peroxy radicals with nitric oxide.

Summary

We have carried out an extensive series of electronic structure calculations primarily at the B3LYP/6-311++G** level on molecular species of relevance to our study of alkyl nitrate yields from the reaction of NO with alkyl peroxy radicals. The species considered are NO, NO_2, alkoxy radicals, alkyl peroxy radicals, alkyl peroxynitrites, and alkyl nitrates, for the cases R =

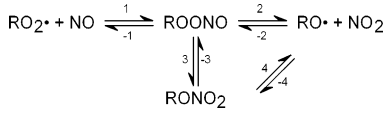

Figure 1. Reaction scheme.

hydrogen, methyl, ethyl, *n*-propyl, isopropyl, and 2-pentyl. Optimized geometries and vibrational frequencies were obtained for each species. Cartesian coordinates in angstroms and vibrational wavenumbers in cm^{-1} from our DFT calculations for RO, RO_2, ROONO, and $RONO_2$ with R = CH_3, C_2H_5, *n*-C_3H_7, *i*-C_3H_7, and 2-C_5H_{11} are available as a Supporting Information table to this paper. Empirical corrections to the calculated DFT energy differences are proposed. We have located very similar transition states for each of the six systems studied. Their energies are high, typically, 140 kJ mol^{-1} (ZPE included) relative to the corresponding peroxynitrites, placing them about 65 kJ mol^{-1} above the energies of the peroxy and NO fragments which initiate the reaction sequence. It is suggested that these barriers must be adjusted downward to account for observed alkyl nitrate yields.

The overall reaction scheme is shown in Figure 1. It is apparent that this is a multiwell, multichannel unimolecular reaction system that is best treated using master equation techniques.[4] The details and results of our reaction simulations will be presented in the following paper[3] in this issue, in which moments of inertia, vibrational frequencies, and corrected energy differences are taken for these simulations from our DFT calculations.

We believe that our DFT studies have provided a very good overall description of the structures and vibrational properties of the alkoxy radicals, alkyl peroxy radicals, alkyl peroxynitrites, and alkyl nitrates, for the cases considered, especially in providing a firm basis for our conclusion that the thermochemistry of these species is essentially independent of the size of the R group, hydrogen being an exception.

Acknowledgment. This project has been supported in part by the American Chemistry Council (through its Atmospheric Chemistry Technical Implementation Panel, contract #0092) and the National Science Foundation (Atmospheric Chemistry Division). The authors particularly thank Timothy J. Wallington for discussions and for a survey of the literature. They also thank Theodore S. Dibble and Joseph S. Francisco for helpful discussions and for sharing computational results. Thanks go to G. Barney Ellison and John F. Stanton for a preprint of their paper and for communicating their results prior to publication. Thanks also go to David M. Golden, Neil Donahue, Geoffrey Tyndall, and John Orlando for discussions. The authors also thank Mr. Jeffrey Brender of the University of Michigan for assistance with the computations.

Supporting Information Available: Table of Cartesian coordinates and vibrational wavenumbers from DFT calculations for RO, RO_2, ROONO, and $RONO_2$ with R = CH_3, C_2H_5, *n*-C_3H_7, *i*-C_3H_7, and 2-C_5H_{11}. This material is available free of charge via the Internet at http://pubs.acs.org.

References and Notes

(1) (a) Atkinson, R. *J. Phys. Chem. Ref. Data*, Monograph 2, 1984. (b) Wallington, T. J.; Nielsen, O. J.; Sehested, J. Reactions of Organic Peroxy Radicals in the Gas Phase in *Peroxy Radicals*; Alfassi, Ed.; Wiley & Sons: New York, 1997.

(2) Arey, J.; Aschmann, S. M.; Kwok, E. S. C.; Atkinson, R. *J. Phys. Chem. A* **2001**, *105*, 1020.

(3) Barker, J. R.; Lohr, L. L.; Reading, S.; Shroll, R. *J. Phys. Chem. A* **2003**, *107*, 7434.

(4) (a) Barker, J. R. *Int. J. Chem. Kinet.* **2001**, *33*, 232; (b) Barker, J. R. MultiWell Program Suite; 1.3.1 ed.; http://aoss.engin.umich.edu/multi-well, Ann Arbor, MI, 2003.

(5) McGrath, M. P.; Francl, M. M.; Rowland, F. S.; Hehre, W. J. *J. Phys. Chem.* **1988**, *88*, 5352.

(6) Morris, V.; Bhatia, S. C.; Hall, J. H., Jr. *J. Phys. Chem.* **1990**, *90*, 7414.

(7) Palmer, M. H. *J. Mol. Struct.* **1990**, *239*, 173.

(8) Koppenol, W.; Klasinc, L. *Int. J. Quantum Chem.: Quantum Biol. Symp.* **1993**, *20*, 1.

(9) McGrath, M. P.; Rowland, F. S. *J. Phys. Chem.* **1994**, *94*, 1061.

(10) Tsai, H.-H. M.; Harrison, J. G.; Martin, J. C.; Hamilton, T. P.; van der Woerd, M.; Jablonsky, M. J.; Beckman, J. S. *J. Am. Chem. Soc.* **1994**, *116*, 4115.

(11) Krauss, M. *Chem. Phys. Lett.* **1994**, *222*, 513.

(12) Cameron, D. R.; Borrajo, A. M. P.; Bennett, B. M.; Thatcher, G. R. J. *Can. J. Chem.* **1995**, *73*, 1627.

(13) Tsai, H.-H.; Hamilton, T. P.; Tsai, J.-H. M.; van der Woerd, M.; Harrison, J. G.; Jablonsky, M. J.; Beckman, J. S.; Koppenol, W. E. *J. Phys. Chem.* **1996**, *100*, 15087.

(14) Jursic, B. S. *J. Mol. Struct. (THEOCHEM)* **1996**, *370*, 65.

(15) Sumathi, R.; Peyerimhoff, S. D. *J. Chem. Phys.* **1997**, *107*, 1872.

(16) Li, Y.; Francisco, J. S. *J. Chem. Phys.* **2000**, *113*, 7976.

(17) Dixon, D. A.; Feller, D.; Zhan, C.-G.; Francisco, J. S. *J. Phys. Chem. A* **2002**, *106*, 3191.

(18) Ellison, G. B.; Blanksby, S. J.; Jochnowitz, E. B.; Stanton, J. F., to be published.

(19) Houk, K. N.; Condroski, K. R.; Pryor, W. A. *J. Am. Chem. Soc.* **1996**, *118*, 13002.

(20) Zhang, D.; Zhang, R.; Park, J.; North, S. W. *J. Am. Chem. Soc.* **2002**, *124*, 9600.

(21) Gaussian 94, Revision B.3, Frisch, M. J.; Trucks, G. W.; Schlegel, H. B.; Gill, P. M. W.; Johnson, B. G.; Robb, M. A.; Cheeseman, J. R.; Keith, T.; Petersson, G. A.; Montgomery, J. A.; Raghavachari, K.; Al-Laham, M. A.; Zakrzewski, V. G.; Ortiz, J. V.; Foresman, J. B.; Peng, C. Y.; Ayala, P. Y.; Chen, W.; Wong, M. W.; Andres, J. L.; Replogle, E. S.; Gomperts, R.; Martin, R. L.; Fox, D. J.; Binkley, J. S.; Defrees, D. J.; Baker, J.; Stewart, J. P.; Head-Gordon, M.; Gonzalez, C.; Pople, J. A. Gaussian, Inc., Pittsburgh, PA 1995.

(22) Hippler, H.; Nasterlack, S.; Striebel, F. *Phys. Chem. Chem. Phys.* **2002**, *4*, 2959.

(23) Becke, A. D. *J. Chem. Phys.* **1993**, *98*, 5648.

(24) He, Y.; Gräfenstein, J.; Kraka, E.; Cremer, D. *Mol. Phys.* **2000**, *98*, 1639.

(25) Lynch, B. J.; Fast, P. L.; Harris, M.; Truhlar, D. G. *J. Phys. Chem.* **2000**, *104*, 4811.

(26) Cremer, D. *Mol. Phys.* **2001**, *99*, 1899.

(27) (a) *CRC Handbook of Chemistry and Physics*, 81st ed.; CRC, 2000. (b) Wagman, D. D.; Evans, W. H.; Parker, V. B.; Schumm, R. H.; Halow, I.; Bailey, S. M.; Churney, K. L.; Nuttall, R. L. *J. Phys. Chem. Ref. Data, Suppl. 2* **1982**, *11*, 1.

(28) Dixon, W. B.; Wilson, E. B., Jr., *J. Chem. Phys.* **1961**, *35*, 191.

(29) Stull, D. R.; Westrum, E. F.; Sinke, G. C. *The Chemical Thermodynamics of Organic Compounds*; Wiley-Interscience: New York, 1969.

(30) Frenkel, M.; Kabo, G. J.; Rogonov, G. N.; Wilhoit, R. C. *Thermodynamics of Organic Compounds in the Gas State*; Thermodynamics Research Center, Texas A & M, College Station, TX, 1994; Vol. 1.

(31) (a) $HONO_2$, NO, NO_2: Ref 27b; (b) OH radical: Ruscic, B.; Feller, D.; Dixon, D. A.; Peterson, K. A.; Harding, L. B.; Asher, R. L.; Wagner, A. F. *J. Phys. Chem. A* **2001**, *105*, 1; (c) HO_2 radical: Bauschlicher, C. W., Jr.; Partridge, H. *Chem. Phys. Lett.* **1993**, *208*, 241.

(32) Francisco, J. S.; private communication.